Sensors & Transducers, Vol. 227, Issue 11, November 2018, pp. 35-41

www.sensorsportal.com

Sensors & Transducers

Published by IFSA Publishing, S. L., 2018
http://www.sensorsportal.com

Tailored Plastic Chip Electrode for Fabrication of Amperometric Glucose Sensor Using GOx@ZIF-8(AuNPs) as Support

[1, 2, *] Anirban Paul, [2] Jibinlal A. and [1, 2, *] Divesh N. Srivsatva

[1] Analytical and Environmental Division and Centralized Instrument Facility, Council of Scientific & Industrial Research (CSIR), Central Salt and Marine Chemicals Research Institute (CSMCRI), G. B. Marg, Bhavnagar-364002, Gujarat, India

[2] Academy of Scientific and Innovative Research (AcSIR), Council of Scientific & Industrial Research (CSIR), Central Salt and Marine Chemicals Research Institute (CSMCRI), G. B. Marg, Bhavnagar-364002, Gujarat, India

[*] E-mail: anirban.paul1989@gmail.com, dnsrivastava@csmcri.res.in

Received: 31 July 2018 /Accepted: 28 September 2018 /Published: 30 November 2018

Abstract: An innovative protocol has been established for the encapsulation of glucose oxidase (GOx) and gold nanoparticles (AuNPs) together into the cavity of ZIF-8 metal organic framework and subsequently utilized for glucose sensing application in aqueous media using plastic chip electrode as an effective platform. ZIF-8 possess high stability both physically and chemically. Its large surface area and tunable cavity size is supportive to accommodate both the GOx and AuNPs. The as-synthesized microstructure is meticulously characterized by various physico-chemical techniques which approves that AuNPs are uniformly distributed within ZIF-8 cavity. The existence of AuNPs not only increases conductivity but also enhance the activity of GOx and enable both glucose oxidation and oxygen reduction reaction in tandem fashion. Plastic chip electrode acts as a superior bulk electrode for fabrication of such glucose sensor in aqueous media. Further, the as synthesized material shows commendable stability with very low-level detection of glucose in aqueous media (60 nM of glucose).

Keywords: Plastic chip electrode, ZIF-8, Gold nanoparticle, Amperometry, Enzymatic glucose sensor.

1. Introduction

Diabetes mellitus is currently considered as one of the most widespread chronic ailments which mainly occurs due to unhealthy lifestyle like obesity and lack of physical activity. The major threat is that it affects blood glucose levels directly which may consequences to serious health issues like kidney failure, cardiac arrest, degeneration of neurons [1]. This solemn threat to health has significantly increased in recent time due to rapid urbanization and hence people acquires such modern lifestyle. Patients having this chronic disease are advised by doctor to monitor their blood glucose level at a regular interval and prescribed insulin shot periodically for long-term management of their blood glucose level [2]. However, available methods of monitoring are associated with pain and troublesome due to possibilities of causing injections. Hence, there is an urgent need for non-invasive glucose monitoring [3-5]. It is almost 55 years passed, since Clark and Lyon first proposed the concept of glucose sensing in 1962 and still there is no sign of diminishing speed of latest technology in this sector. More generally, the advancement of amperometric glucose sensor devices

till 1962 can be separated into three generations. First-generation devices were based on the simple principle which is consumption of the atmospheric O_2 co-substrate and the production of H_2O_2 which was to be detected as a function of glucose concentration. Second generation devices had been prepared by substituting atmospheric O_2 with another electron mediator. Latest third generation devices have mainly focused with non-invasive mediator free detection of glucose from saliva/sweat. This whole voyage of advancement has been extensively reviewed by various authors [6-8]. The most vital and fundamental concept to develop mediator free glucose biosensor is to facilitate direct electron transfer between the electrode and the active centre of redox protein [9]. Although, the task is rather difficult to accomplish as the redox active protein (Flavin adenine dinucleotide [FAD]/$FADH_2$) and the prosthetic group of glucose oxidase (GOX) are deeply buried inside the rigid and non-conducting layer of GOX. Electron mediator species is thus utilized externally to facilitate this catalytic reaction artificially [9-10].

Scientific community shows promising interest over metal organic framework (MOF) due to its large surface area, unique design, and most importantly uniform and tuneable pore sizes [11]. Zinc-imidazole framework 8 (ZIF-8), classified under zeolitic MOF, was reported to be an excellent chemical moiety having specific pore size to accommodate small to large biomolecule and protect them from major external stimuli [12-20]. Metal nanoparticles (MNPs), in the other hand, possess excellent chemical and physical properties and a useful tool to fabricate mediator free biosensor. Generally MNPs have been used frequently to design such biosensor for twin purpose as it significantly increases the surface conductance of the electrode to mediate charge easily to the electrode surface and in the same time, enhances the surface area so that the electron tunnelling distance is sufficiently low for mediating of charge [21-26]. Recent reports of Dong, *et al*. shows preparation of ZIF-8 nanostructure composite, encapsulated with GOx and PVP stabilized NiPd as an effective catalyst for glucose sensing [27]. Among numerous nanoparticles, Au nanoparticles (AuNPs), stabilized by citrate, shows promising interest to scientific community due to its exceptional properties. One of this is high conductivity of AuNPs which helps to mediate charge from the electrolyte to electrode surface. Another important reason to choose AuNPs is due to highly dispersed in water causing zero interference with biological species [28-31]. Plastic chip electrode, a cheap and viable bulk conducting electrode, had been fabricated by our group few years ago and till now it is extensively used for various of applications in the field of chemistry and biology. It is an important opportunity to avoid costly electrode to fabricate biosensors as the viability of PCE is proved to be exactly same compared to other market available electrodes.

In this work, we report the applicability of plastic chip electrode to fabricate a mediator free glucose sensor. synthesis of GOx@ZIF-8(AuNPs) by encapsulation of gold nanoparticles and glucose oxidase together into the cavity of ZIF-8 and utilize for the catalytic oxidation of glucose. Citrate stabilized Au nanoparticle was synthesized and reported in our previous work [32]. Here it has been encapsulated successfully onto ZIF-8 matrix along with glucose oxidase. The catalyst was utilized in amperometric glucose sensor having a detection limit as low as 60 nM of glucose, accrediting glucose monitoring from sweat. In sort, the present catalytic protocol is more efficient and robust for the low-level detection of glucose (60 nM) in aqueous media based on our knowledge.

2. Experimental

2.1. Materials and methods

All the chemicals were of analytical grade and used without further purification. $HAuCl_4.3H_2O$, trisodium citrate dehydrate, Glucose oxidase from aspergillus niger (GO_x), 2-Methylimidazole were purchased from sigma Aldrich and used as received. $Zn(NO_3)_2.6H_2O$ was purchased for SRL chemicals and used as received. GO_x@ZIF-8(AuNPs) nanocomposite was synthesized at room temperature in aqueous media. To prepare GO_x@ZIF-8(AuNPs) nanocomposite, AuNPs and GO_x (aspergillus niger) were added in the reaction mixture of the ZIF8- metal organic framework.

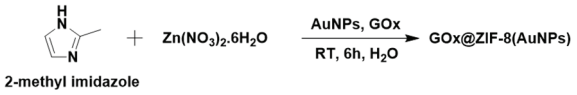
Plastic chip electrode was prepared in reported method and had been used for all electrochemical experiments. The electrode was rinsed with ultrapure water and dried at room temperature. All the experiments were done in three electrode electrochemical setups comprising PCE as working, Pt wire (0.1 mm diameter) as a counter and Ag/AgCl (sat. KCl) as a reference electrode. All the electrochemical measurement was by Metrohm Autolab 302 potentiostat/galvanostat. The GOx@ZIF-8(AuNPs) slurry was prepared by dispersing 10 mg of material in 1mL of pH 7.4 buffer and sonicated for 15 minutes. 10 µL of as prepared solution was drop-casted over PCE surface. 5 µL 0.5 % nafion is added to the mixture as a binder.

The crystal structure of the product was characterized by XRD (PAN Analytical Empyrean Series 2 X-ray diffraction system). The morphology and microstructure of the synthesized materials were investigated by FESEM (JEOL JSM-7100F,) and HRTEM (JEOL JEM-2100). FT-IR was done at Parkin-Elmer G-FTIR. Detail synthetic procedure of GO_x@ZIF-8(AuNPs) nanocomposite is as follows. For all electrochemical measurement Metrohm Autolab 302 potentiostat/galvanostat is used.

2.2. Synthesis of GO_x@ZIF-8(AuNPs)

ZIF-8 was synthesized by previous reported method. 23 gm of 2-methlyimidazole (109 mili moles)

was taken in 420 mL of ultrapure mili-Q water. 50 mg of GOx (8170 units in 50mg) was added in the same solution. This mixture turned pale yellow in colour due to dissolved GO_x and labelled (A). 1.20 gm of $Zn(NO_3)_2.6H_2O$ (1.54 mili moles) was dissolved in another 380 mL of ultrapure milli-Q water separately and labelled (B) Gold nanoparticles (AuNPs) were prepared by our previously reported protocol [32]. Trisodium citrate dehydrate was used as stabilizing as well as reducing agent in aqueous media. As synthesized AuNPs were stored at 4˚C temperature for further use. 10 mL of citrate stabilized AuNPs was taken separately (C). The mixture of B & C was added to the mixture A under constant stirring of 700 rpm at room temperature and the reaction mixture was continuously stirred for 3 hours. In the very beginning of the reaction, solution was transparent and yellow in colour which started to turn hazy after few minutes of stirring. After completion of 3 hours the mixture was allowed to stand for overnight and then supernatant was decanted. It has been observed that the yellow colour of the mixture disappeared after the successive addition but no deep red colour of AuNPs appeared. This give initial confirmation on encapsulation of both GO_x and AuNPs together inside ZIF-8 moiety. The settled solid part was centrifuged and washed with 50 mL of water for 3 times to remove any excess GO_x and AuNPs (not encapsulated). Further it was dried under vacuum and purple colour solid composite was recovered, preferably assumed the formation of GO_x@ZIF-8(AuNPs) nanocomposite. The synthesized probe was characterized by FT-IR, Powder XRD, FE-SEM, STEM to confirm the artefact. The scheme is depicted below in Scheme 1.



Scheme 1. Preparation of Gox@ZIF-8(AuNPs).

2.3. Tailoring of Plastic Chip Electrode

Plastic chip electrode was fabricated in reported method [33]. A simple composite of 60:40 of graphite and poly methyl methacrylate (PMMA) was taken in chloroform. For this case, we had prepared a composite of 6 g of graphite powder and 4 g of PMMA in 25 mL of chloroform. The composite was stirred constantly with a glass rod and ultrasonicated for 15 minutes. A thick slurry of graphite-PMMA composite was poured into a specific template (10 cm × 10 cm glass plate) containing a lamination sheet and dried overnight. The bulk electrode was peeled out from the template and cut into pieces having a size of 3 cm × 0.8 cm (length × width). A circular area of 5 mm diameter was cut in a lamination sheet by plotter cutter and respective electrode was placed to that circular area and lamination was done using a laminator to get fixed surface area having 5 mm diameter. The fabricated electrode was washed with milli-Q water for immobilization of catalyst. 10 µL of as synthesized material, dispersed in pH 7.4 buffer, was drop-casted and dried in room temperature. 5 µL of 0.5 % nafion is added for firm binding of the material to electrode surface. Further, the tailored electrode was utilized for amperometric measurement.

3. Results and Discussions

3.1. Characterization of Materials

The citrate stabilized AuNPs and GO_x inside ZIF-8 material shows very distinctive structural features. Its phase was determined by X-Ray powder diffraction (P-XRD) after vacuum drying. P-XRD pattern of as synthesized GO_x@ZIF-8(AuNPs), is shown in the Fig. 1 (red colour) and is compared with the simulated powder XRD data of the ZIF-8 (blue colour), furnished in same figure. It is clearly observed that the P-XRD peaks of the synthesized GO_x@ZIF-8(AuNPs) matches well with the simulated ZIF-8, indicating no change in the native structural property of the ZIF-8 due to encapsulation of AuNPs and GO_x. As synthesized GO_x@ZIF-8(AuNPs) has been confirmed by its cubic shape (JCPDS: 00-062-1030, $a = b = c =$ 17.0116 Å, $\alpha = \beta = \gamma =$ 90°).

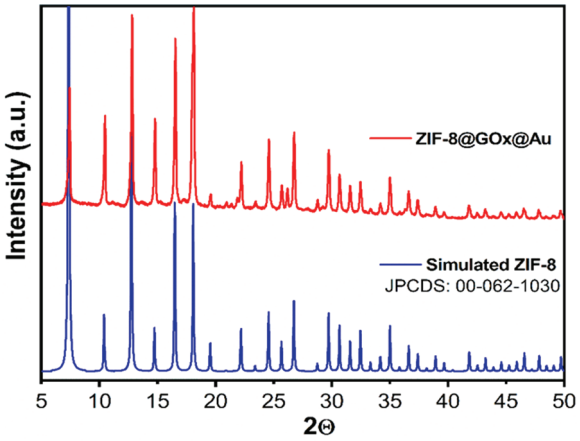


Fig. 1. XRD patterns for simulated ZIF-8 (JCPDS: 00-062-1030) and as synthesized GOx@ZIF-8(AuNPs).

The morphology of GO_x@ZIF-8(AuNPs) was examined by field-emission scanning electron microscopy (FESEM). Fig. 2(a) represents assembled star shaped morphology of ZIF-8 microstructure at low magnification. Whereas high magnified FE-SEM image shows assembly of rod like star morphology (Fig. 2(b)). GO_x has definitely played a crucial role in controlling the morphologies as GO_x has an affinity towards imidazole containing building block (ZIF-8) arises from intermolecular H-bonding and hydrophobic interaction [27]. Further, TEM was performed for detailed investigation of the synthesized microstructure and is depicted in Fig. 2(c). The image

shows the presence of highly crystalline distinctive lattice fringes, probably due to plane of Au nanoparticles over the surface of ZIF-8 moiety which also perfectly correlates with the XRD result. For further investigation, R-TEM was performed and upon increasing the resolution, (111) plane of Au was observed which also correlated with P-XRD data.

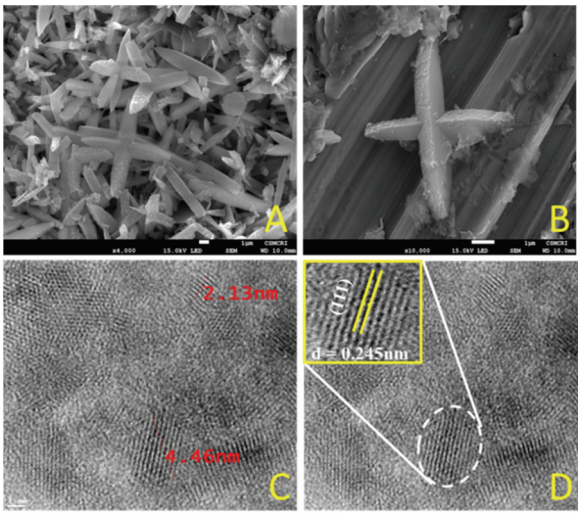


Fig. 2. FESEM image of 5 nm gold coated GO_x@ZIF-8(AuNPs) (a) crystalline growth (b) single particle showing large surface area (c) High resolution HRTEM image of Au lattice fringes (d) STEM-EDX line profile of GOx@ZIF-8(AuNPs) showing almost equal distribution of AuNPs.

To, prove the presence of GO_x in its native structure inside the ZIF8 cavity, Fourier Transform Infrared Spectroscopy (FT-IR) had been performed. GO_x has characteristic IR peaks at 1647 and 1426 cm^{-1} due to stretching vibration of –C=O group present in peptidic bond of amide-I and in-plane bending vibration of N_5H in FAD group respectively [34]. It is clearly seen from Fig. 3 that 1654 cm^{-1} peak of amide-I is slightly shifted to 1647 cm^{-1} as it is highly sensitive towards the structural modification [35].

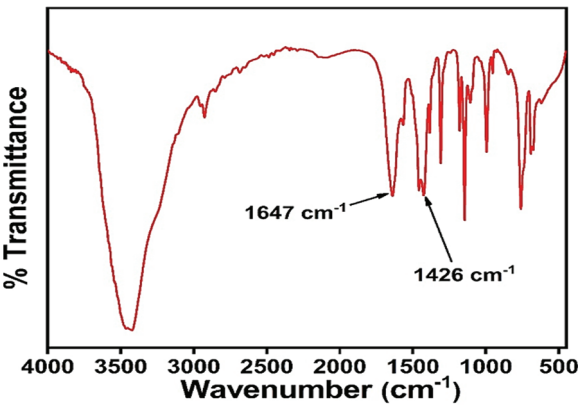


Fig. 3. FTIR Spectra of GO_x@ZIF-8(AuNPs)possessing two distinguishable peaks at 1647 cm^{-1} for -C=O stretching of Amide I and 1426 cm^{-1} for plane bending of FAD group.

Presence of both peaks at 1647 and 1426 cm^{-1} signify the presence of GO_x. These results clearly suggest that the GO_x does not degrade and possess its native structure inside the cavity of ZIF-8, showing biocatalytic activity.

3.2. Electrochemistry of GOx@ZIF-8(AuNPs)

Cyclic voltammetry (CV) measurement was carried out at a scan rate of 50 mV/S to evaluate the electrochemical property of GO_x@ZIF-8(AuNPs). For this purpose, three composites: ZIF-8, GOx@ZIF-8 and GO_x@ZIF-8(AuNPs) were scanned potentiodynamically. Prior to use, PCE was sonicated in milli-Q water for 15 minutes and then then dried at room temperature. 5 mg of each composite was dispersed in 1 mL of 0.1 M pH 7.4 PBS buffer by ultrasonication for 10 minutes and 10 µM from the aliquot was drop casted onto the PCE having a diameter of 5 mm. The electrode was kept covered to avoid external dust and was stored overnight at room temperature for drying. The modified electrode, projected as working electrode, was then immersed in N_2 saturated 0.1 M pH 7.4 PBS buffer for CV measurement. Pt wire (0.1 mm diameter) was taken as a counter electrode, whereas Ag/AgCl (sat. KCl) was taken as a reference electrode. CV was measured in the range of -0.2 to -0.7 V vs Ag/AgCl (sat. KCl) at a scan rate of 50 mV/S. Relatively higher scan rates are always preferred to assess the reversibility of electrochemical reaction. The result is depicted in Fig. 4. Both the ZIF-8 and GOx@ZIF-8 exhibits typical non-faradaic capacitive nature due to double layer capacitance and hence indicative of absence of any redox species (Fig. 4, red and blue dashed lines).

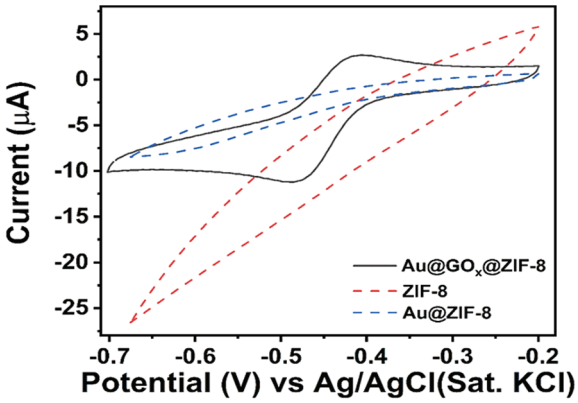


Fig. 4. Cyclic Voltammetry of ZIF-8@GO_x (blue dashed line), ZIF-8 (red dashed line) and GO_x@ZIF-8(AuNPs)(Black line) at a scan rate of 0.05 V/S in N_2 saturated 0.1M pH 7.4 PBS.

CV response of GO_x@ZIF-8(AuNPs) composite shows immense faradaic behaviour with visible sharp peaks in both cathodic and anodic potential at

E_{pa}= - 414 mV and E_{pc}= - 474 mV, having a peak separation of ΔE_p= 60 mV, which is consistent with reported value of E_{pa}= - 419 mV and E_{pc}= - 473 mV, [9] represents significantly high electron transfer rate of the reversible redox equilibrium of the FAD/$FADH_2$ redox couple. The encapsulation of Au nanoparticle is thus playing an importance role, not only by shortening the electron tunnelling distance but also increasing the sensitivity of the system upto 10-folds. The surface plasmon resonance energy of Au nanoparticle is so high that it can establish effective interaction with biomolecules resulting an immense increment in the output [36].

3.3. Calibration Plot

The amperometric measurement was performed in potentiostatic method. The experiment had performed by successive addition of 10 mM glucose to the air saturated pH 7.4 buffer solution at a characteristic potential of – 0.47 V vs Ag/AgCl (sat. KCl) (Fig. 5). Stair shaped change in current had been observed with quick steady state upon successive addition of glucose had been observed upon zooming, had been depicted inset of Fig. 5. The change of current creates a drift and the drift became stable after certain time due to formation of H_2O_2. Calibration plot is considered to be one of the most important characteristics of an electrochemical sensor and to do so the steady state current had been plotted with the concentration. A two-slope plot has been obtained due to formation and saturation of H_2O_2 formed. The result is depicted in Fig. 6.

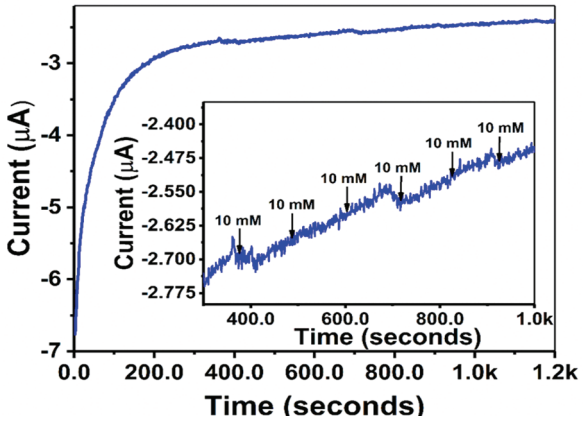


Fig. 5. Typical steady state amperometric measurement of catalytic glucose oxidation at -0.45 V vs Ag/AgCl (sat. KCl) with successive addition of 0.1 mM glucose. Calibration plot of concentration versus (full and linear region) current has been depicted inset.

Two different slopes with two different regression coefficients had been observed. Both the coefficients show excellent linearity of the fabricated sensor. A low-level detection of 60 nM of glucose had been observed for this biosensor which is quite good for such point of view to detect glucose from sweat/saliva. Moreover, we have used plastic chip electrode which is also extremely chip platform for detection rather than conventional costly electrodes. We observed that the current achieved steady state gradually after 15 successive dilution. The reason behind achieving such steady state is due to the increment of dissolved oxygen which disturbs the equilibrium of FAD/$FADH_2$. Although This low detection limit can be attributed to our claim of measuring blood glucose from sweat which encourages non-invasive, point of the care device.

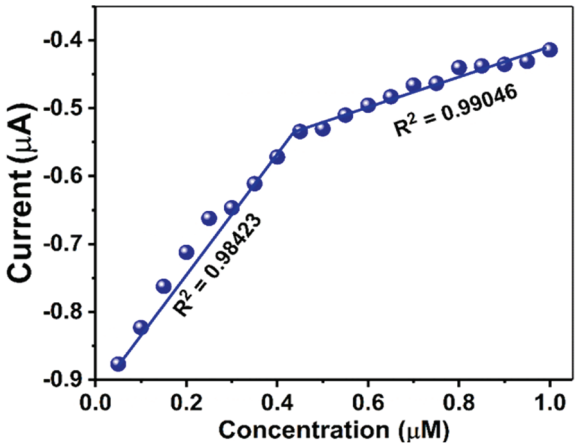


Fig. 6. Calibration plot of estimation of glucose concentration showing two distinct slopes having excellent regression coefficients.

4. Conclusions

In this paper, we have encapsulated AuNPs and GOx inside and ZIF -8 cavity and the synthesized composite is drop-casted over homemade plastic chip electrode for detection of glucose. The as synthesized composite was synthesized in gram scale and can be up scale to any desired limit. The composite material was thoroughly characterized by various physico chemical techniques. The characterization reveals that the synthesized material is highly crystalline in nature AuNPs is well dispersed, inside very stable framework. The presence of highly conducting AuNPs and GO_x on GOx@ZIF-8(AuNPs) nanocomposite, facilitate the consecutive oxidation of glucose. Plastic chip electrode had been used for first time for any biosensor application which will be a landmark for the preparation of economical biosensor preparation. Presence of Au nanoparticle increases the sensitivity of the system upto 10-fold with low level of glucose detection *i.e.* 60 nM in aqueous media. The result can be accredited towards fabrication of non-invasive glucose sensor mainly from sweat/saliva. Overall, the present methodology demonstrates an efficient, robust, economical and tolerable nanocomposite for glucose sensing in aqueous media by electrochemical pathway and can be an excellent alternative of market available glucose sensor.

Acknowledgements

CSIR funded project (MLP-0018) is thankfully acknowledged for financial support. AP is thankful to CSIR for senior research fellowship. CSMCRI-AESD and CIF is acknowledged for all the instrumental facilities.

References

[1]. Whiting D. R., Guariguata L., Weil C., Shaw J., IDF diabetes atlas: global estimates of the prevalence of diabetes for 2011 and 2030, *Diabetes Res. Clin. Pract.,* Vol. 94, Issue 3, 2011, pp. 311–321.

[2]. Moncada S., Higgis A., The L-arginine-nitric oxide pathway, *N Engl J Med.,* Vol. 329, Issue 27, 1993, pp. 2002–2012.

[3]. Gao W., Emaminejad S., Nyein H. Y. Y., Challa S., Chen K., Peck A., Fahad H. M., Ota H., Shiraki H., Kiriya D., Lien D. H., Brooks G. A., Davis R. W., Javey A., Fully integrated wearable sensor arrays for multiplexed in situ perspiration analysis, *Nature,* Vol. 529, Issue 7587, 2016, pp. 509–514.

[4]. Lee H., Choi T. K., Lee Y. B., Cho H. R., Ghaffari R., Wang L., Choi H. J., Chung T. D., Lu N., Hyeon T., Choi S. H., Kim D. H., A graphene-based electrochemical device with thermoresponsive microneedles for diabetes monitoring and therapy, *Nat. Nanotechnol.,* Vol. 11, Issue 6, 2016, pp. 566–572.

[5]. Bandodkar A. J., Jia W., Yardimci C., Wang X., Ramirez J., Wang J., Tattoo-based noninvasive glucose monitoring: a proof-of-concept study, *Anal. Chem.,* Vol. 87, Issue 1, 2015, pp. 394–398.

[6]. Rahman M. M., Ahammad A. J. S., Jin J.-H., Ahn S. J., Lee J.-J., A comprehensive review of glucose biosensors based on nanostructured metal-oxides, *Sensors,* Vol. 10, Issue 5, 2010, pp. 4855–4886.

[7]. Wang J., Glucose biosensors: Forty years of advances and challenges, *Eletroanalysis,* Vol. 13, Issue 12, 2001, pp. 983–988.

[8]. Wang J., Electrochemical glucose biosensors, *Chem. Rev.,* Vol. 108, Issue 2, 2008, pp. 814–825.

[9]. Bao S.-J., Li C. M., Zang J.-F., Cui X.-Q., Qiao Y., Guo J., New Nanostructured TiO_2 for Direct Electrochemistry and Glucose Sensor Applications, *Adv. Funct. Mater.,* Vol. 18, Issue 4, 2008, pp. 591–599.

[10]. Liu J., He Z., Khoo S. Y., Tan T. T. Y., A new strategy for achieving vertically-erected and hierarchical TiO_2 nanosheets array/carbon cloth as a binder-free electrode for protein impregnation, direct electrochemistry and mediator-free glucose sensing, *Biosens. Bioelectron.,* Vol. 77, 2016, pp. 942–949.

[11]. Furukawa H., Cordova K. E., O'Keeffe M., Yaghi O. M., The chemistry and applications of metal-organic frameworks, *Science,* Vol. 341, Issue 6149, 2013.

[12]. Zhong H. X., Wang J., Zhang Y. W., Xu W. L., Xing W., Xu D., Zhang Y. F., Zhang X. B., ZIF-8 Derived Graphene-Based Nitrogen-Doped Porous Carbon Sheets as Highly Efficient and Durable Oxygen Reduction Electrocatalysts, *Angew. Chemie - Int. Ed.,* Vol. 53, Issue 51, 2014, pp. 14235–14239.

[13]. Pan Y., Liu Y., Zeng G., Zhao L., Lai Z., Rapid synthesis of zeolitic imidazolate framework-8 (ZIF-8) nanocrystals in an aqueous system, *Chem. Commun.,* Vol. 47, Issue 7, 2011, pp. 2071-2073.

[14]. Lu G., Hupp J. T., Metal−Organic Frameworks as Sensors: A ZIF-8 Based Fabry−Pérot Device as a Selective Sensor for Chemical Vapors and Gases, *J. Am. Chem. Soc.,* Vol. 132, Issue 23, 2010, pp. 7832–7833.

[15]. Banerjee R., Furukawa H., Britt D., Knobler C., O'Keeffe M., Yaghi O. M., Control of Pore Size and Functionality in Isoreticular Zeolitic Imidazolate Frameworks and their Carbon Dioxide Selective Capture Properties, Journal of the American Chemical Society, *J. Am. Chem. Soc.,* Vol. 131, Issue 11, 2009, pp. 3875–3877.

[16]. Liu H., Liu Y., Li Y., Tang Z., Jiang H., Metal−Organic Framework Supported Gold Nanoparticles as a Highly Active Heterogeneous Catalyst for Aerobic Oxidation of Alcohols, *J. Phys. Chem. C,* Vol. 114, 2010, pp. 13362–13369.

[17]. Wang B., Côté A. P., Furukawa H., O'Keeffe M., Yaghi O. M., Colossal cages in zeolitic imidazolate frameworks as selective carbon dioxide reservoirs, *Nature,* Vol. 453, Issue 7192, 2008, pp. 207–211.

[18]. Lu G., Li S., Guo Z., Farha O. K., Hauser B. G., Qi X., Wang Y., Wang X., Han S., Liu X., Duchene J. S., Zhang H., Zhang Q., Chen X., Ma J., Loo S. C. J., Wei W. D., Yang Y., Hupp J. T., Huo F., Imparting functionality to a metal-organic framework material by controlled nanoparticle encapsulation, *Nat. Chem.,* Vol. 4, Issue 4, 2012, pp. 310–316.

[19]. Banerjee R., Phan A., Wang B., Knobler C., Furukawa H., O'Keeffe M., Yaghi O. M., High-throughput synthesis of zeolitic imidazolate frameworks and application to CO_2 capture, *Science,* Vol. 319, Issue 5865, 2008, pp. 939–943.

[20]. Hu Y., Liao J., Wang D., Li G., Fabrication of gold nanoparticle-embedded metal-organic framework for highly sensitive surface-enhanced Raman scattering detection, *Anal. Chem.,* Vol. 86, Issue 8, 2014, pp. 3955–3963.

[21]. Liu S., Ju H., Reagentless Glucose Biosensor Based on Direct Electron Transfer of Glucose Oxidase Immobilized on Colloidal Gold Modified Carbon Paste Electrode, *Biosens. Bioelectron.,* Vol. 19, Issue 3, 2003, pp. 177–183.

[22]. Zhai D., Liu B., Shi Y., Pan L., Wang Y., Li W., Zhang R., Yu G., Highly sensitive glucose sensor based on pt nanoparticle/polyaniline hydrogel heterostructures, *ACS Nano,* Vol. 7, Issue 4, 2013, pp. 3540–3546.

[23]. Sakslund H., Wang J., Lu F., Hammerich O., Development and evaluation of glucose microsensors based on electrochemical codeposition of ruthenium and glucose oxidase onto carbon fiber microelectrodes, *J. Electroanal. Chem.,* Vol. 397, Issue 1–2, 1995, pp. 149–155.

[24]. Mazeiko V., Kausaite-Minkstimiene A., Ramanaviciene A., Balevicius Z., Ramanavicius A., Gold Nanoparticle and Conducting Polymer-Polyaniline-Based Nanocomposites for Glucose Biosensor Design, *Sensors Actuators B: Chem.,* Vol. 189, 2013, pp. 187–193.

[25]. Gao Z. Da, Guo J., Shrestha N. K., Hahn R., Song Y. Y., Schmuki P., Nickel hydroxide nanoparticle activated semi-metallic TiO_2 nanotube arrays for non-enzymatic glucose sensing, *Chem. - A Eur. J.,* Vol. 19, Issue 46, 2013, pp. 15530–15534.

[26]. Luo W., Zhu C., Su S., Li D., He Y., Huang Q., Fan C., Self-Catalyzed, Self-Limiting Growth of Glucose

Oxidase-Mimicking Gold Nanoparticles, *ACS Nano,* Vol. 4, Issue 12, 2010, pp. 7451–7458.
[27]. Wang Q., Zhang X., Huang L., Zhang Z., Dong S., GOx@ZIF-8(NiPd) Nanoflower: An Artificial Enzyme System for Tandem Catalysis, *Angew. Chemie - Int. Ed., 130022*, 2017, pp. 16082–16085.
[28]. Bai Y., Yang W., Sun Y., Sun C., Enzyme-free glucose sensor based on a three-dimensional gold film electrode, *Sensors Actuators B: Chem.,* Vol. 134, Issue 2, 2008, pp. 471–476.
[29]. Bharathi S., Nogami M., A glucose biosensor based on electrodeposited biocomposites of gold nanoparticles and glucose oxidase enzyme, *Royal Society of Chemistry,* Vol. 126, Issue 11, 2001, pp. 1919–1922.
[30]. Xu M., Song Y., Ye Y., Gong C., Shen Y., Wang L., Wang L., A novel flexible electrochemical glucose sensor based on gold nanoparticles/polyaniline arrays/carbon cloth electrode, *Sensors Actuators B: Chem.,* Vol. 252, 2017, pp. 1187–1193.
[31]. Luo X. L., Xu J. J., Du Y., Chen H. Y., A glucose biosensor based on chitosan–glucose oxidase–gold nanoparticles biocomposite formed by one-step electrodeposition, *Anal. Biochem.,* Vol. 334, Issue 2, 2004, pp. 284–289.
[32]. Maity D., Kumar A., Gunupuru R., Paul P., Colorimetric detection of mercury(II) in aqueous media with high selectivity using calixarene functionalized gold nanoparticles, *Colloids Surfaces A: Physicochem. Eng. Asp.,* Vol. 455, Issue 1, 2014, pp. 122–128.
[33]. Perween M., Parmar D. B., Bhadu G. R., Srivastava D. N., Polymer-graphite composite: a versatile use and throw plastic chip electrode, *Analyst,* Vol. 139, Issue 22, 2014, pp. 5919–5926.
[34]. Gutierrez F., Rubianes M. D., Rivas G. A., Dispersion of multi-wall carbon nanotubes in glucose oxidase: Characterization and analytical applications for glucose biosensing, *Sensors Actuators B: Chem.,* 2012, Vol. 161, Issue 1, pp. 191–197.
[35]. Hereć M., Gagoś M., Kulma M., Kwiatkowska K., Sobota A., Gruszecki W. I., Secondary structure and orientation of the pore-forming toxin lysenin in a sphingomyelin-containing membrane, *Biochim. Biophys. Acta - Biomembr.,* Vol. 1778, Issue 4, 2008, pp. 872–879.
[36]. Kumar A., Bhatt M., Vyas G., Bhatt S., Paul P., Sunlight Induced Preparation of Functionalized Gold Nanoparticles as Recyclable Colorimetric Dual Sensor for Aluminum and Fluoride in Water, *ACS Appl. Mater. Interfaces,* Vol. 9, Issue 20, 2017, pp. 17359–17368.

Published by International Frequency Sensor Association (IFSA) Publishing, S. L., 2018 (http://www.sensorsportal.com).

